Plasma Reactions of O_n High Energy Species – O, O_2(v), $O_2(a\ ^1\Delta_g)$, and O_3

O_2 plasma kinetics workshop
Reykjavik
Sep 2016

Albert A. Viggiano
Space Vehicles Directorate
Air Force Research Laboratory

Outline

- Brief introduction to ionospheric chemistry
  - Reasons for energetic oxygen studies

- Techniques for O, $O_2(v)$, $O_2(a\ ^1\Delta_g)$, and O_3

- Data examples for each reactant

Summary of Main Ionospheric Chemistry of N and O species

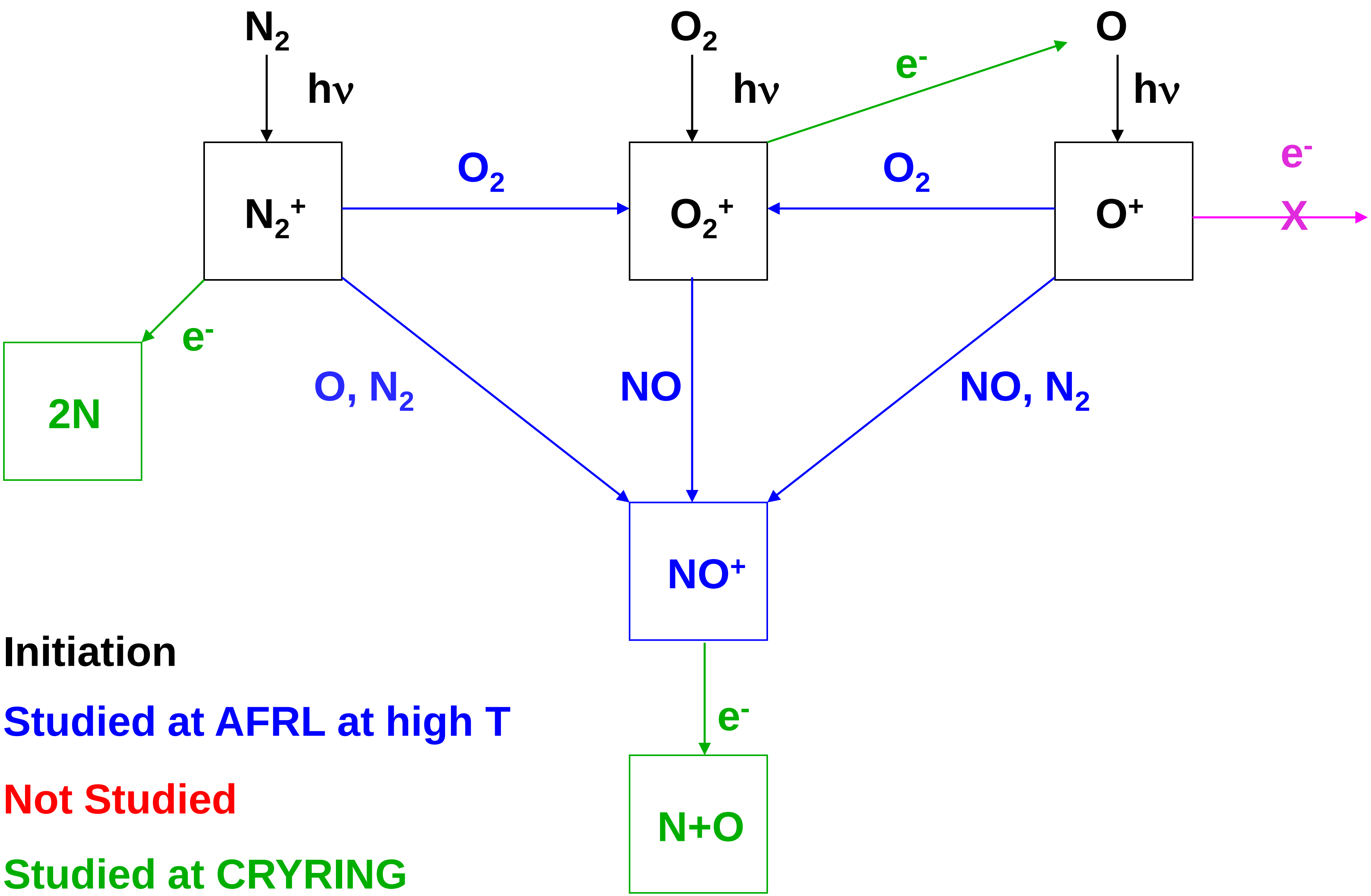

Negative Ion Reactions in the Atmosphere

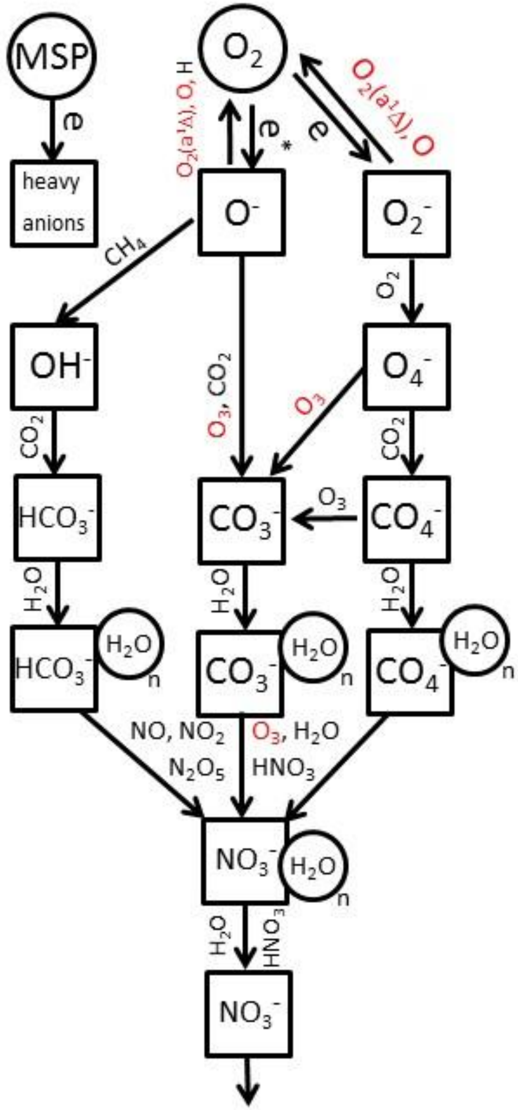

Numerous places reactive oxygen species are important

For more information on atmospheric ion chemistry Chem. Rev. ***115***, 4542–4570 (Feb 2015)

Hypersonic Plasma Effects

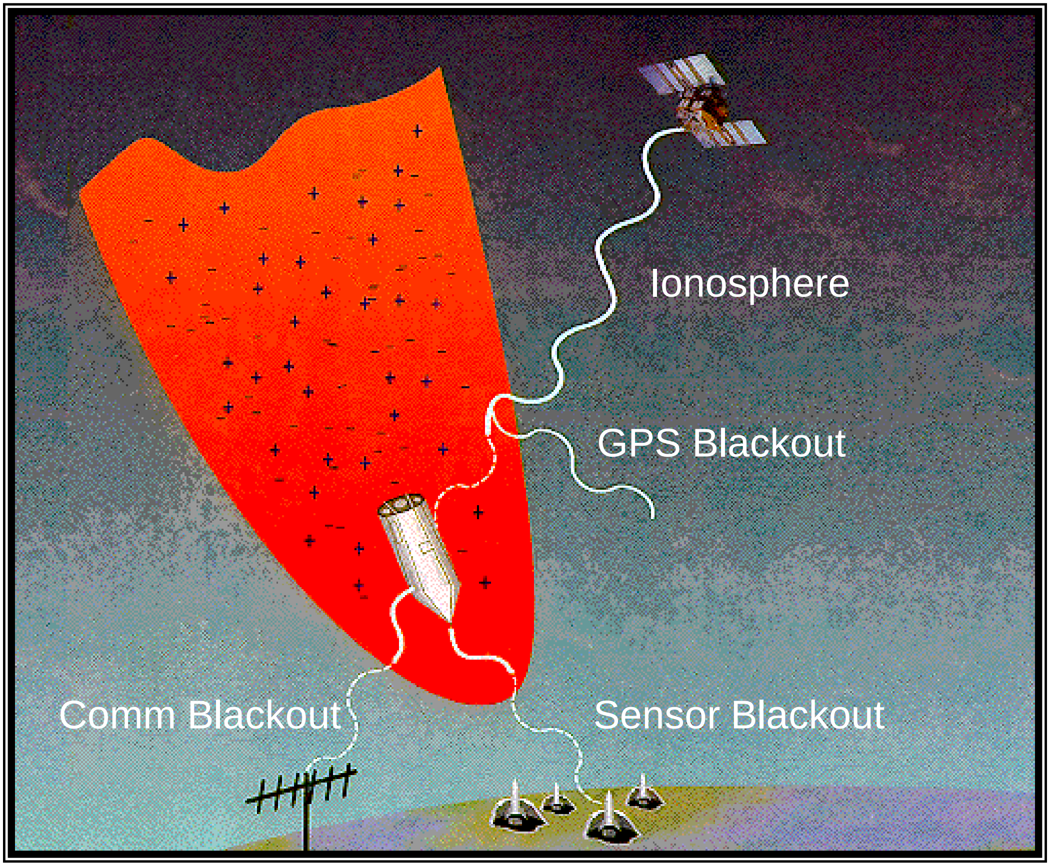

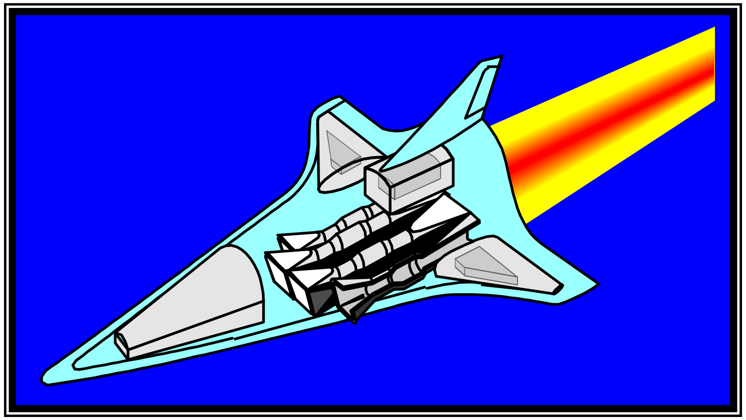

- AJAX hypersonic concept vehicle utilizes air plasmas to aid combustion
- Plasma Blackout of C^3I, GPS Navigation

Combustor Test @ Mach 2

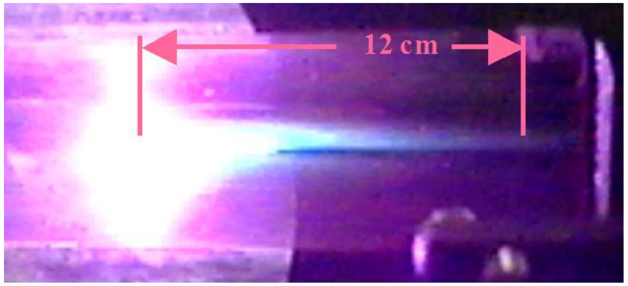

Selected Ion Flow Tube (SIFT) for $O_2(v)$

- T Range 85 - 550 K
- Pressure Range ~0.3 - 1 Torr
- Kinetic energy range 0.01 – 1eV

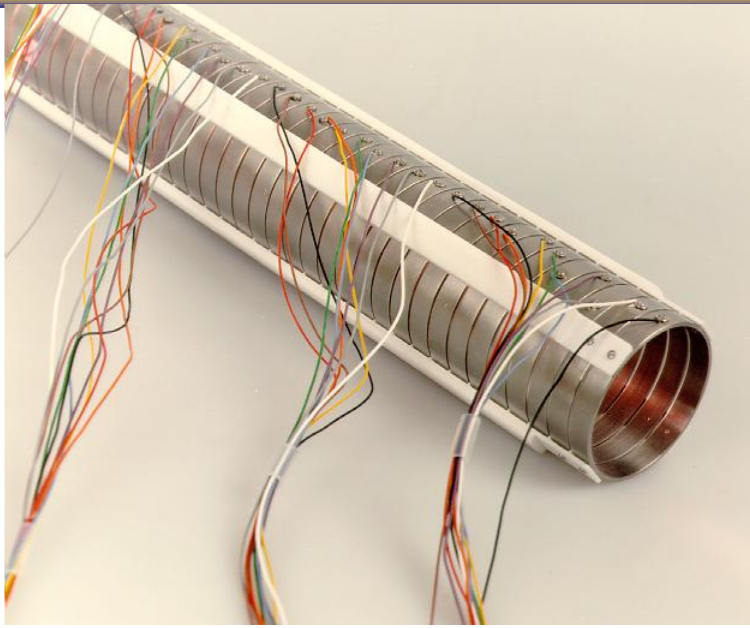

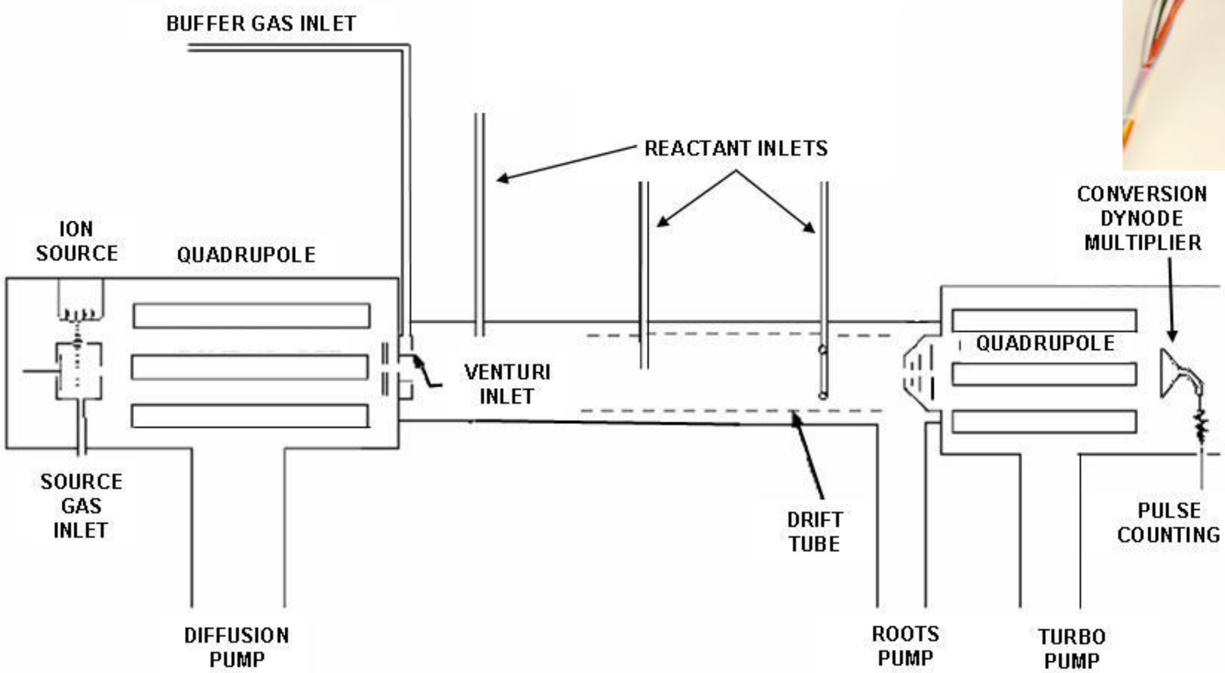

Important:

Translational energy distribution is Quasi-Boltzmann

High Temperature Flowing Afterglow (HTFA)

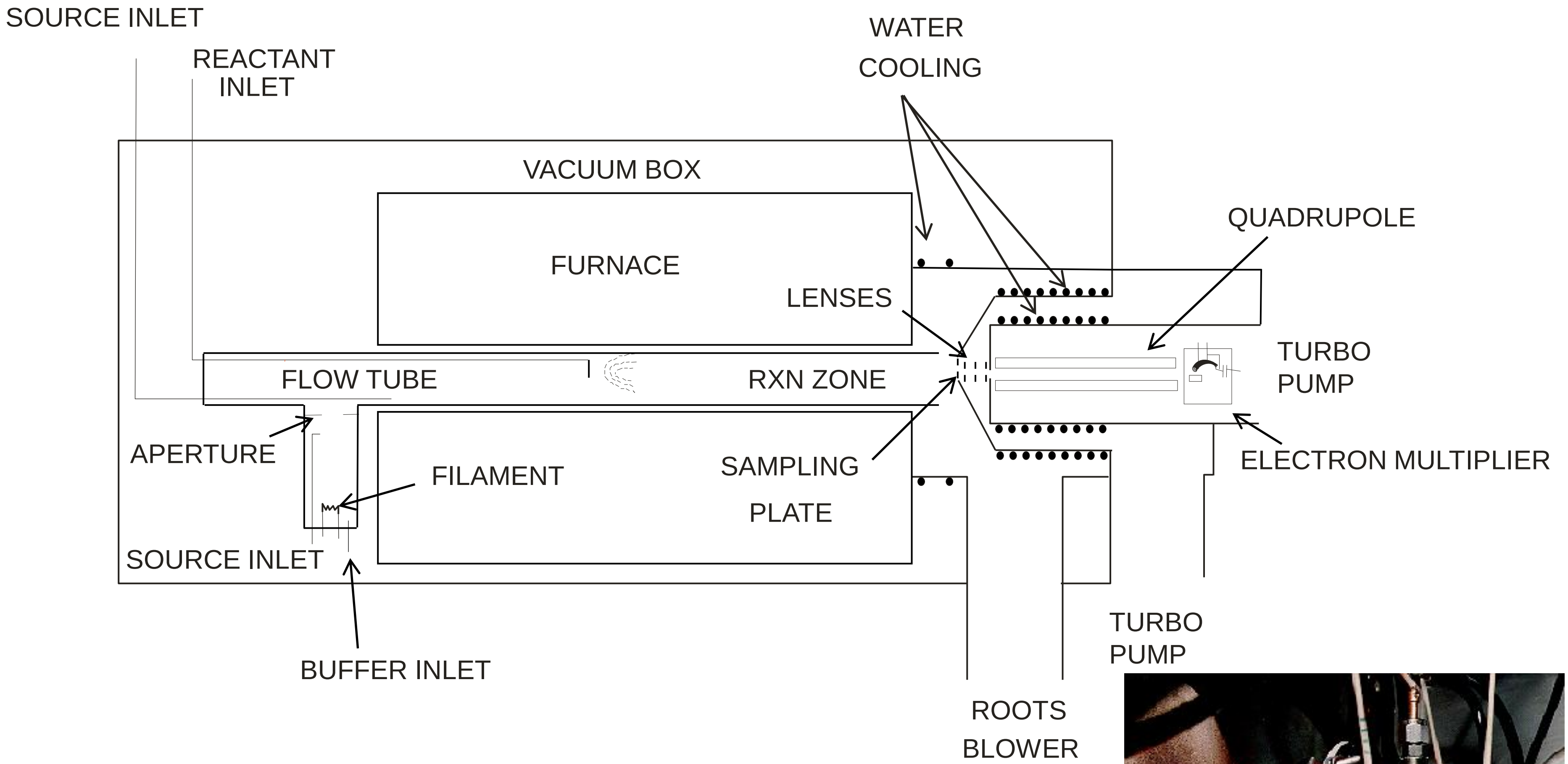

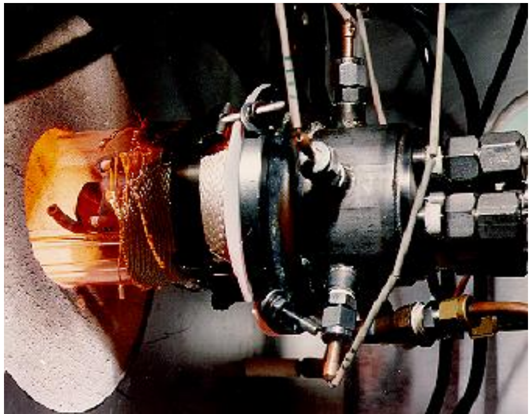

Temperature Range 300-1800 K

Ceramic tube - 1800 K

Quartz tube - 1400 K

Data from HTFA and Drift Tube → Internal Energy Dependence

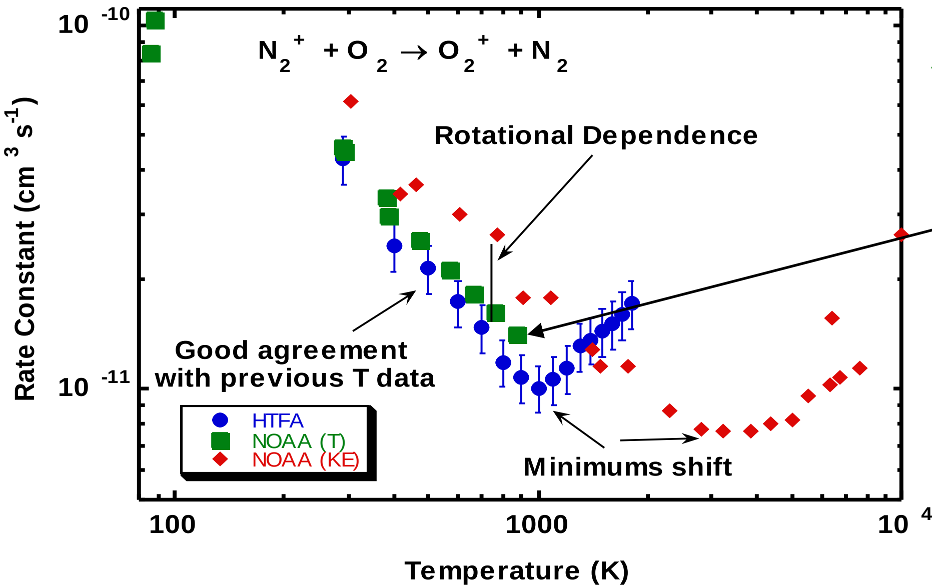

vs. T or KE

900 K limitation miss upturn

Add rotational energy

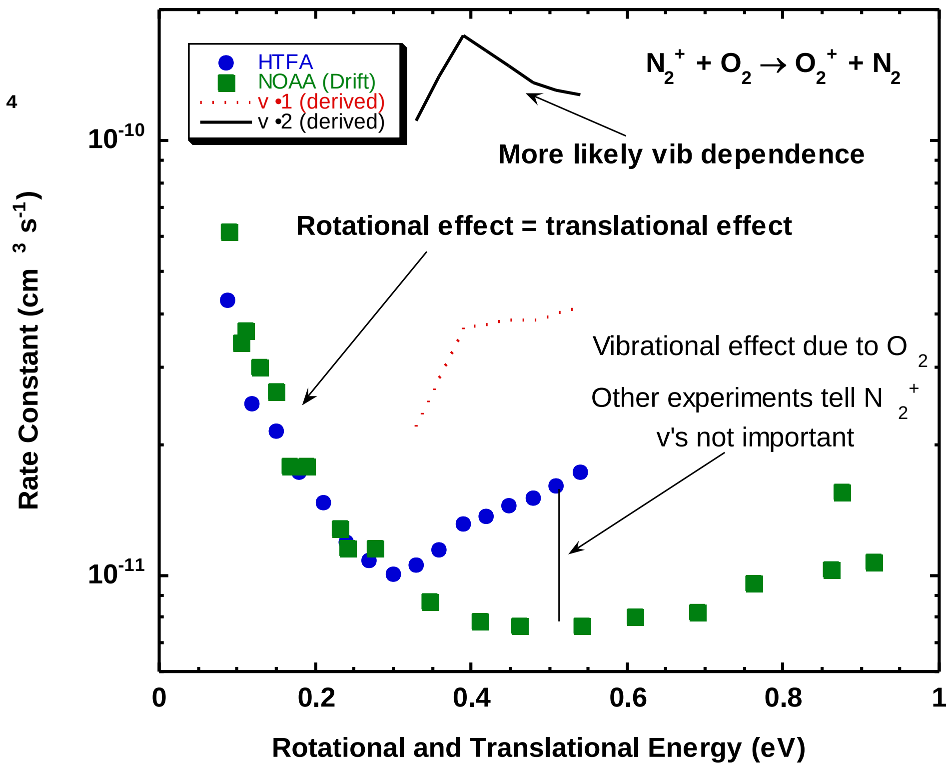

Most Important Ionospheric Reactions

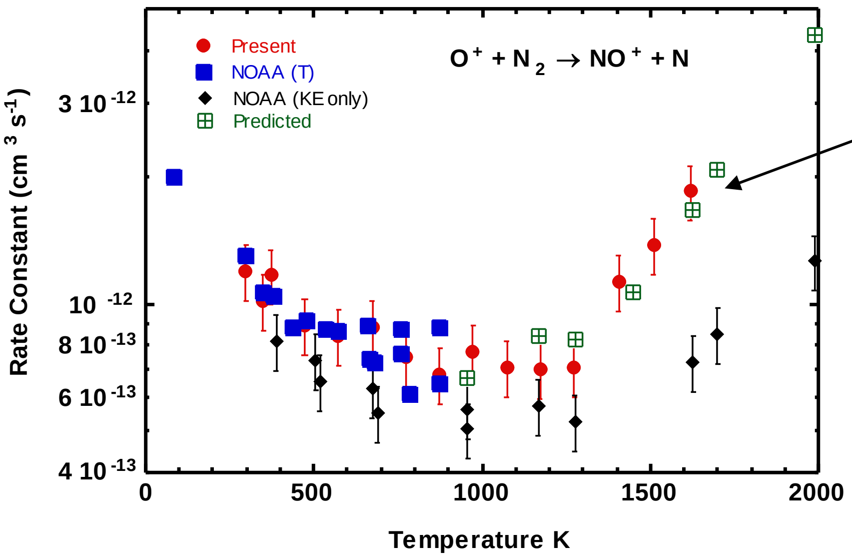

Changes directions at 900 K
Upturn vs T mostly N_2 (v≥2)
Previous data missed upturns

Big difference between T and KE
Vibrationally excited O_2 important
maybe 10x faster for v = 2

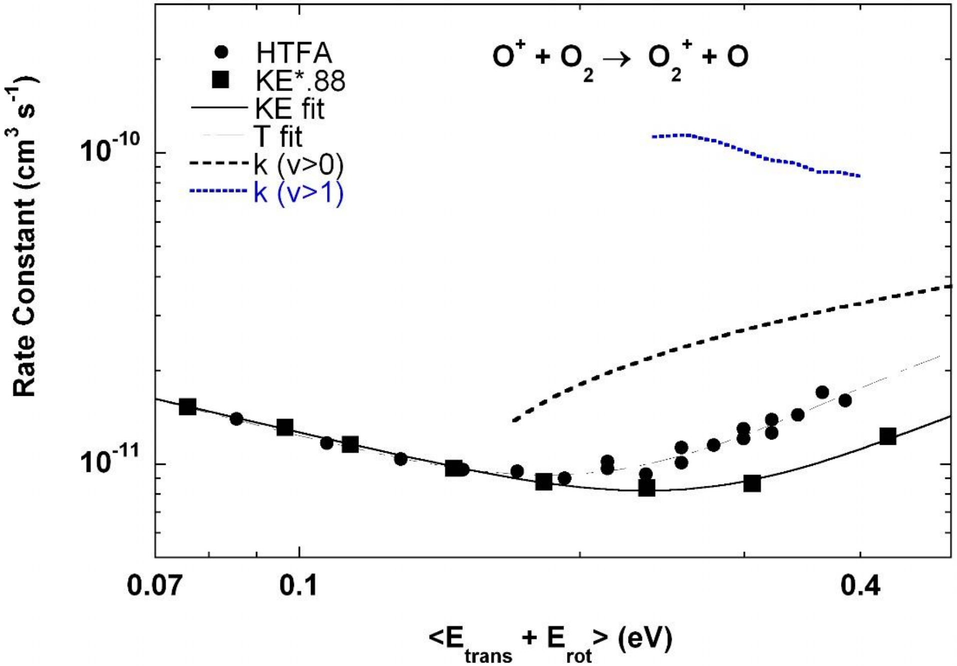

N, O Reactions Studied at AFRL by this technique

See: Adv. in Gas Phase Ion Chem. vol. 4, **p 85-136 (Dec 2001)**

$O^+ + O_2 \rightarrow O_2^+ + O$ (≤ 1800 K)

$O^+ + N_2 \rightarrow NO^+ + N$ (≤ 1600 K) most important reaction in ionosphere

$O^+ + NO \rightarrow NO^+ + O$ (≤ 1400 K)

$O_2^+ + NO \rightarrow NO^+ + O$ (≤ 1400 K)

$N_2^+ + O_2 \rightarrow O_2^+ + N_2$ (≤ 1800 K)

$N^+ + O_2 \rightarrow NO^+, O_2^+, O^+$ (≤ 1400 K) also product sates of NO^+

$N_n^+ + NO \rightarrow$ products (≤ 1400 K)

$N_3^+ + O_2 \rightarrow NO^+; NOO^+$ (≤ 1400 K)

Chemistry of NOO^+

$O_3^+ + N_2, O_2 \rightarrow$ products

Ionospheric Data (with E. Mishin, B. Burke)

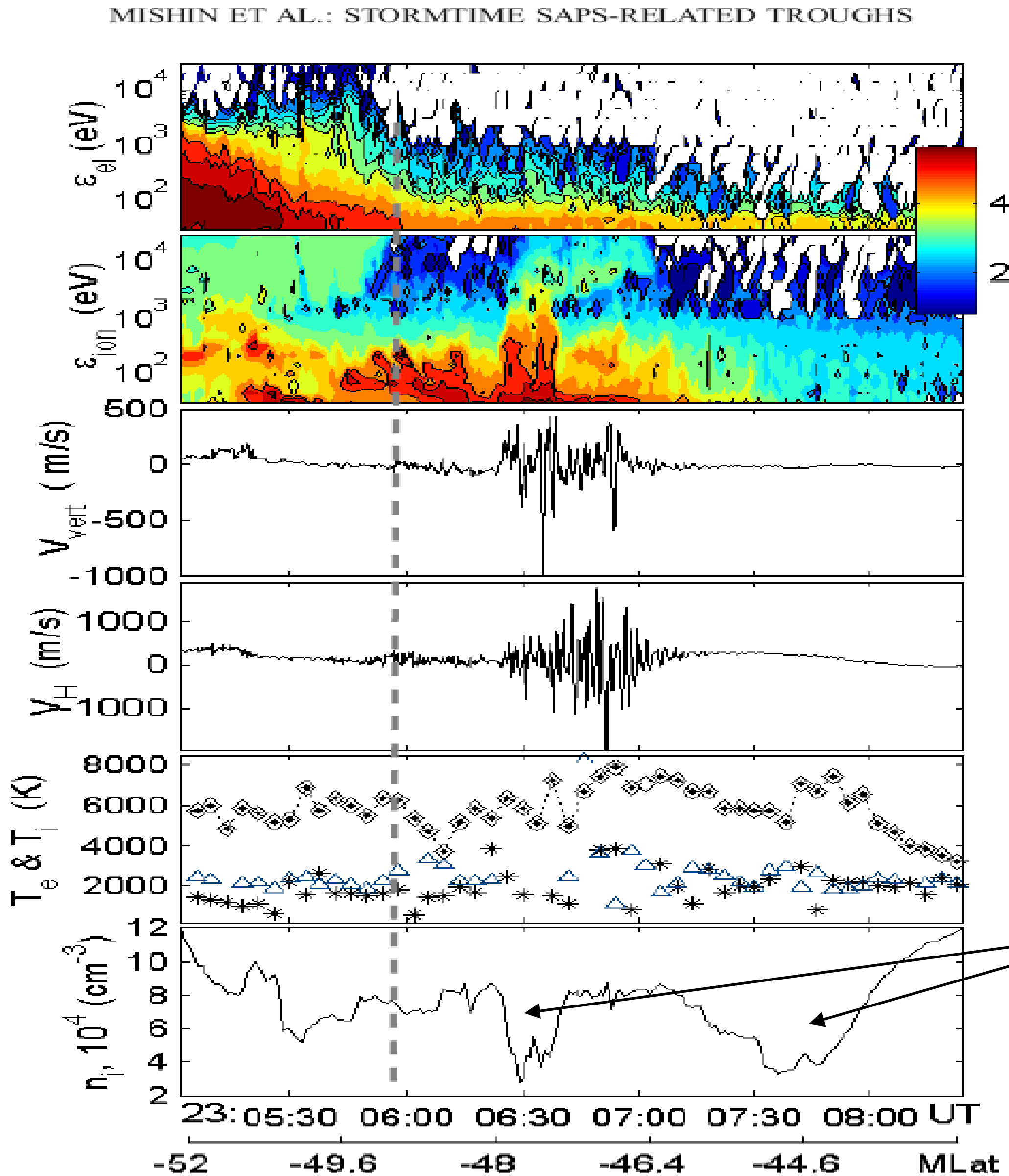

SAPS wave structure observed by DMSP F14 at 2307 UT on 6 April 2000

Density trough

Ionospheric Depletion Data

$(n_i - n_i^{max}) / n_i^{max}$

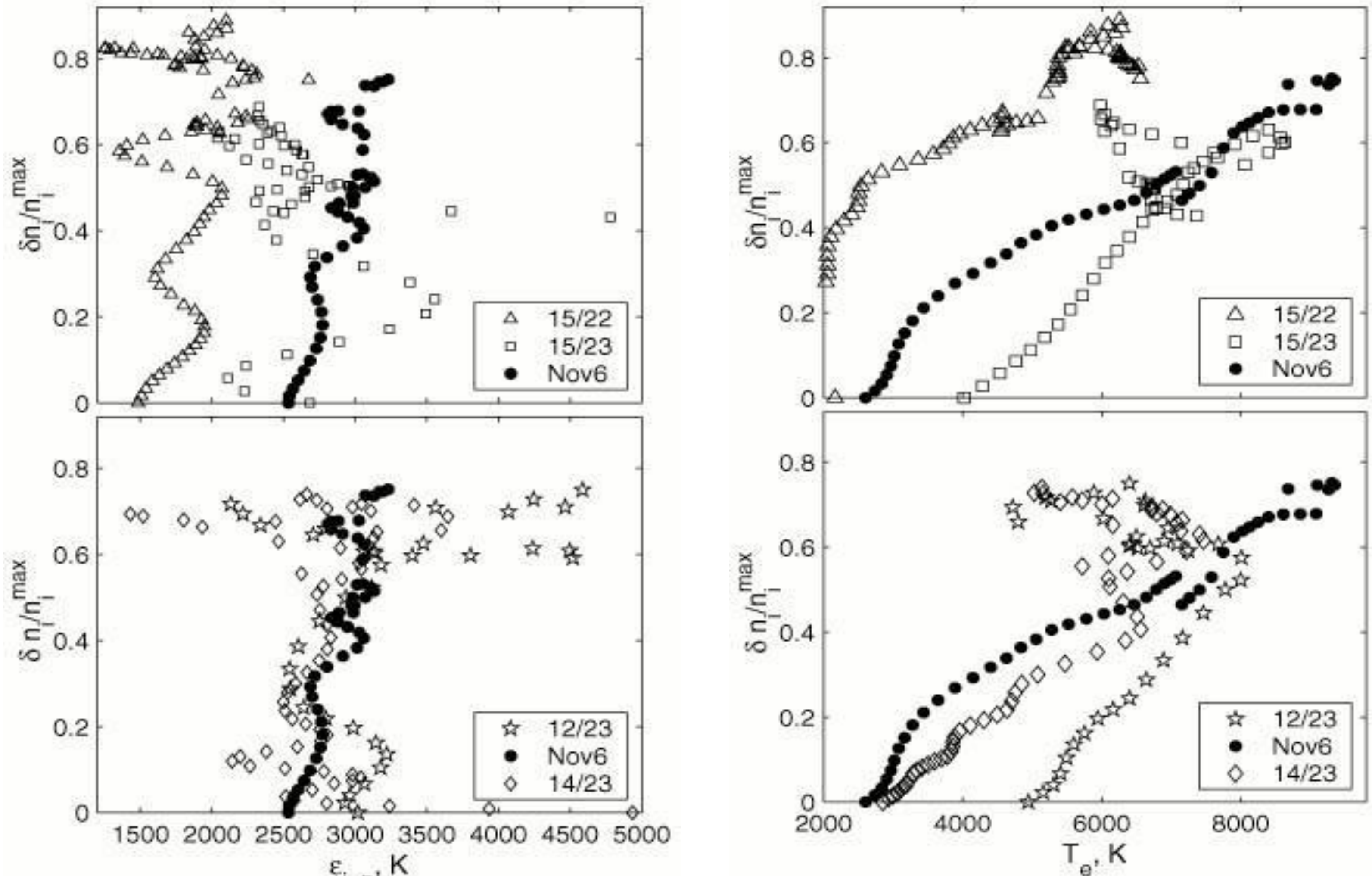

Ion Temperature **Electron temperature**

Dependence on electron temperature was not expected

Chemistry Leading to Trough

Vibrational excitation

$e(KE) + N_2 \rightarrow N_2(v)$

$e(KE) + O_2 \rightarrow O_2(v)$

More KE ⇒ more vib.

Atom Transfer

$O^+ + N_2(v) \rightarrow NO^+ + N$

Charge Exchange

$O^+ + O_2(v) \rightarrow O_2^+ + O$

More vib. ⇒ k faster

Uses HTFA data

Dissociative Recombination

$NO^+ + e \rightarrow O + N$

$O_2^+ + e \rightarrow O + O$

More diatomic ⇒ more recomb.

Our data shows that vibrational excitation leads to faster conversion of atomic species (non-recombining) to diatomic species (recombining)

Determines the ionization balance in the F region

$N^+ + O_2$ Chemistry Studied

- Rate constants to 1400 K
  - Rotational and translational energy do little to change rate or products
  - v = 1 goes at $k_{langevin}$
- Three products formed
  - ~50% O_2^+ (CT)
  - ~40% NO^+
  - ~10% O^+
- All NO^+ is ground state ($^1\Sigma$) even though NO^+ ($^3\Sigma$) is exothermic (300- 550 K)

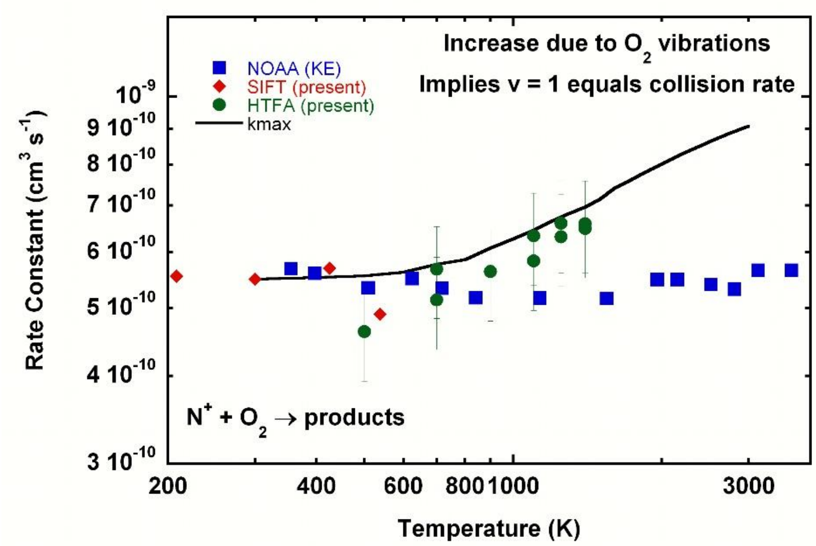

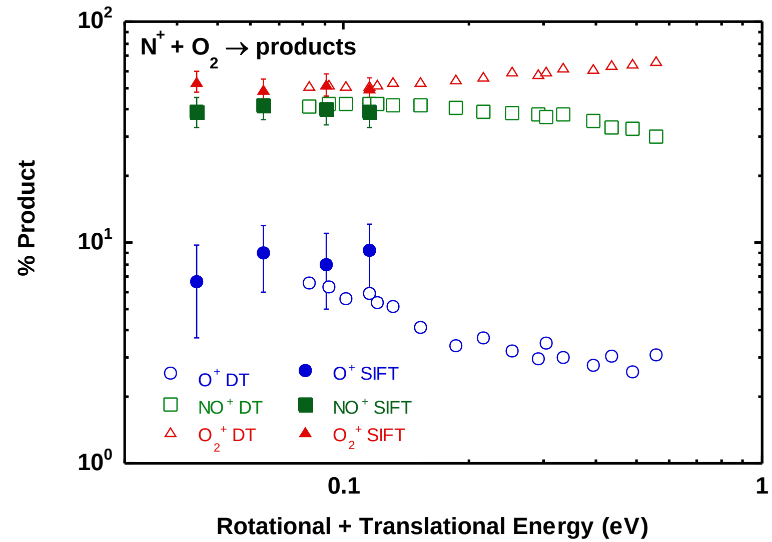

Instruments for ion and electron molecule studies of O_3

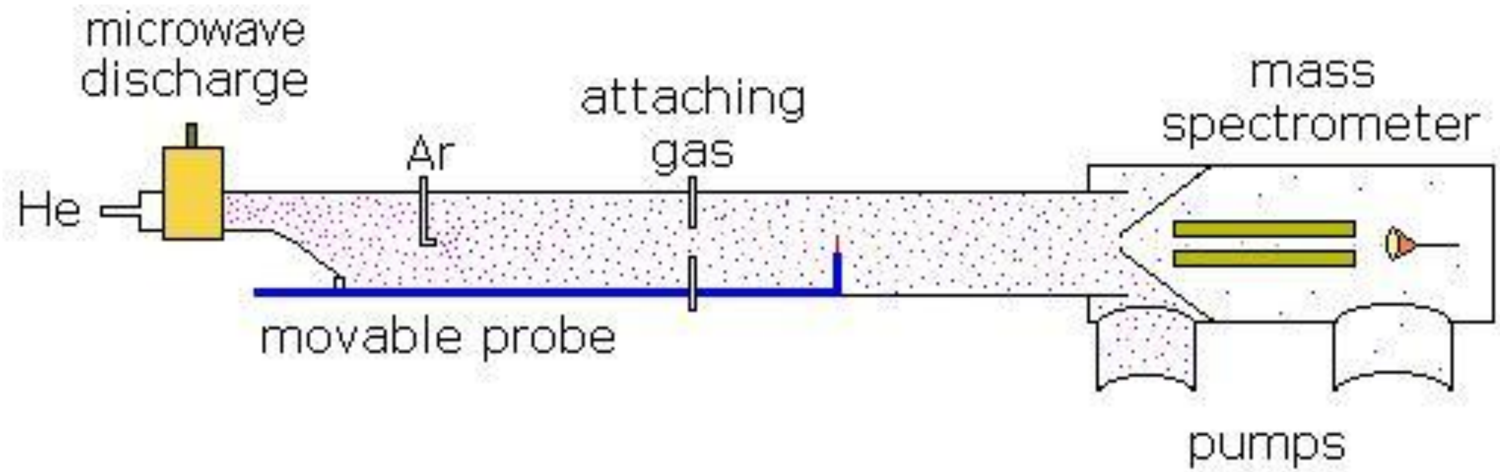

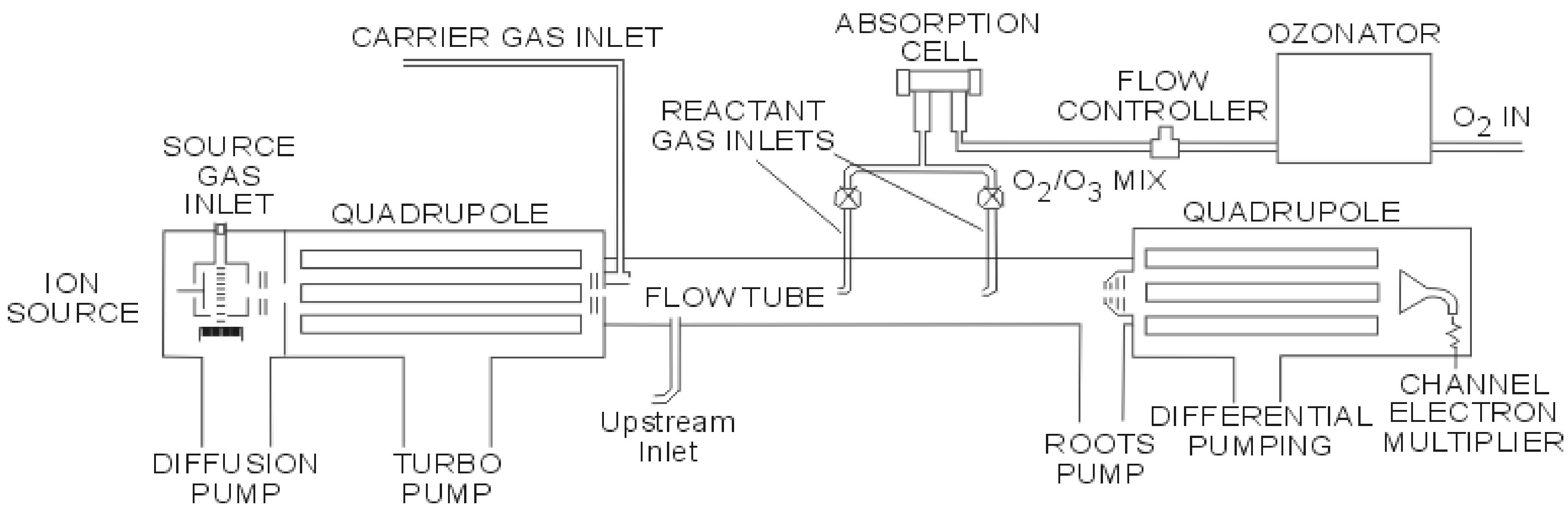

Atmospheric Ozone Reactions

J. Phys. Chem. A; *106*(6), 997-1003 (Jan 2002)

TABLE 1: Reaction Rate Constants for Reactions of Ozone at 300 K Measured with the Selected Ion Flow Tube (SIFT)[a]

reaction	products	k;[k_c] (10^{-9} cm^3 s^{-1})	branching fractions	$-\Delta H$ kJ/mol
$O^- + O_3 \rightarrow$		*1.7*;[*1.5*]		
	$O_3^- + O$		0.81	63
	$O_2^- + O_2$		0.19	294
$O_2^- + O_3 \rightarrow$	$O_3^- + O_2$	*1.3*;[*1.2*]	1.00	160
$OH^- + O_3 \rightarrow$		*1.4*;[*1.4*]		
	$O_3^- + OH$		0.90	28
	$HO_2^- + O_2$		0.08	100
	$O_2^- + HO_2$		0.02	47
$NO_2^- + O_3 \rightarrow$		*0.18*;[*1.1*]		
	$NO_3^- + O_2$		0.99	264
	$O_3^- + NO_2$		0.01	−14
$NO_3^- + O_3 \rightarrow$	no reaction	<*0.005*;[*0.97*]		
	$NO_2^- + 2O_2$			21
$CO_3^- + O_3 \rightarrow$	no reaction	<*0.001*;[*0.98*]		
	$O_2^- + CO_2 + O_2$			98
$CO_4^- + O_3 \rightarrow$		*0.46*;[*0.93*]		
	$O_3^- + CO_2 + O_2$		0.93	81
	$CO_3^- + 2O_2$		0.07	108

$e^- + O_3$

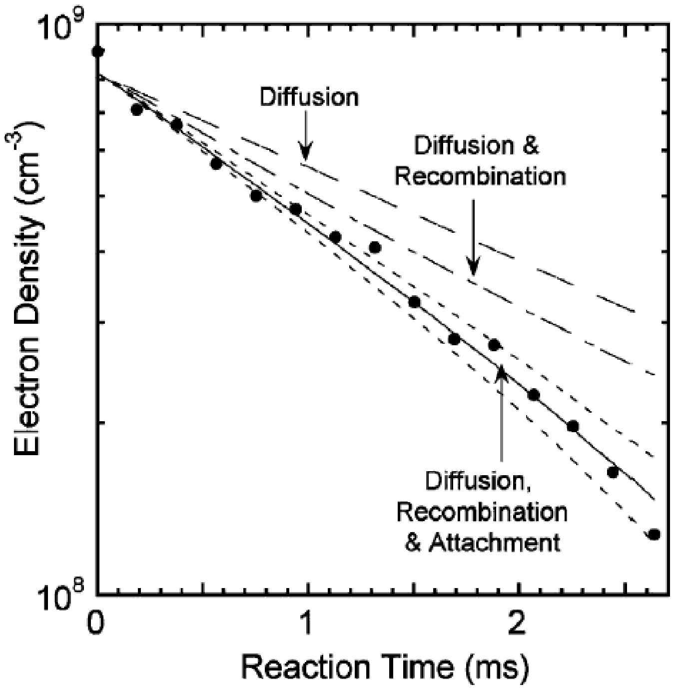

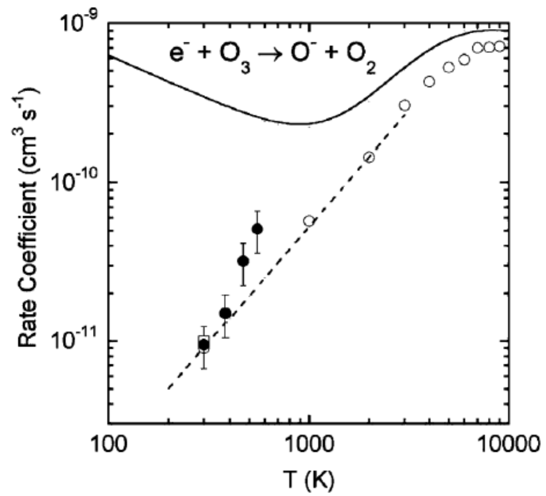

FIG. 2. Electron attachment rate coefficient versus temperature. Present results (●) and swarm upper limit of Fehsenfeld *et al.* [3] (□) are true thermal values. The remaing data are plotted versus electron temperature. The drift tube results of Stelman *et al.* [4] (dashed line) are derived from a least squares fit of the combined data for 200 and 300 K rovibrational temperature ozone reacting with energetic electrons. The electron beam results of Skalny *et al.* [8] (○) and Senn *et al.* [2] (solid line) were derived by those authors from measurements of the reaction cross section for 300 K rovibrational temperature ozone with energetic electrons.

Phys. Rev. Lett. **91** DOI: 223201 -1-4 (Nov 2003). 1

O, N atom reaction technique

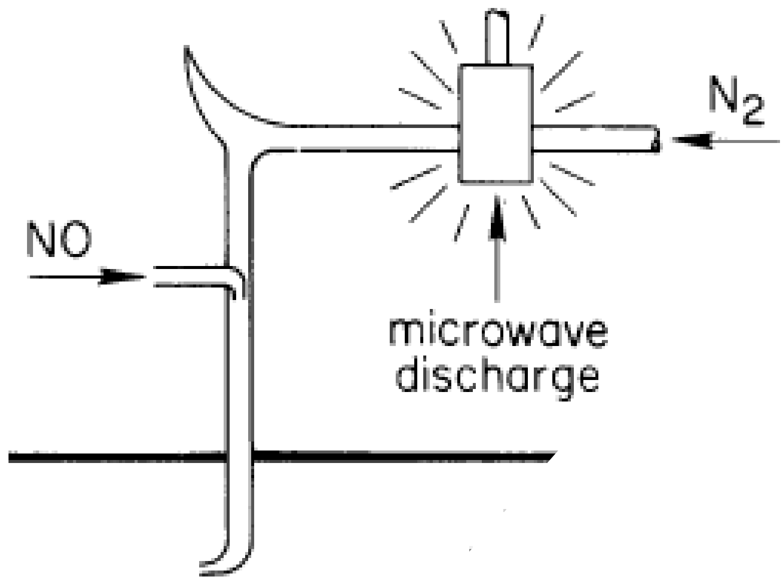

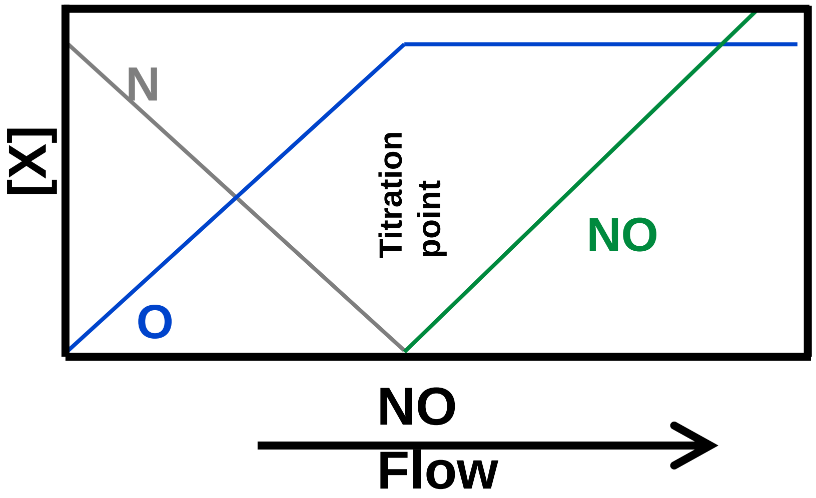

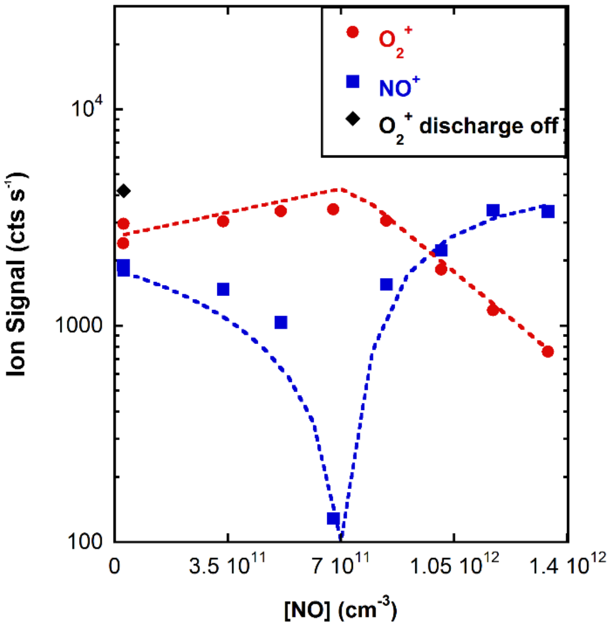

Positive Ion - Atom Results

$O_2^+ + N \rightarrow NO^+ + O$ $\Delta H_r^0(0K) = -96.5$ kcal/mol (1)

$N_2^+ + O \rightarrow NO^+ + N$ $\Delta H_r^0(0K) = -70.6$ kcal/mol (2a)

$\rightarrow N_2 + O^+$ $\Delta H_r^0(0K) = -45.2$ kcal/mol (2b),

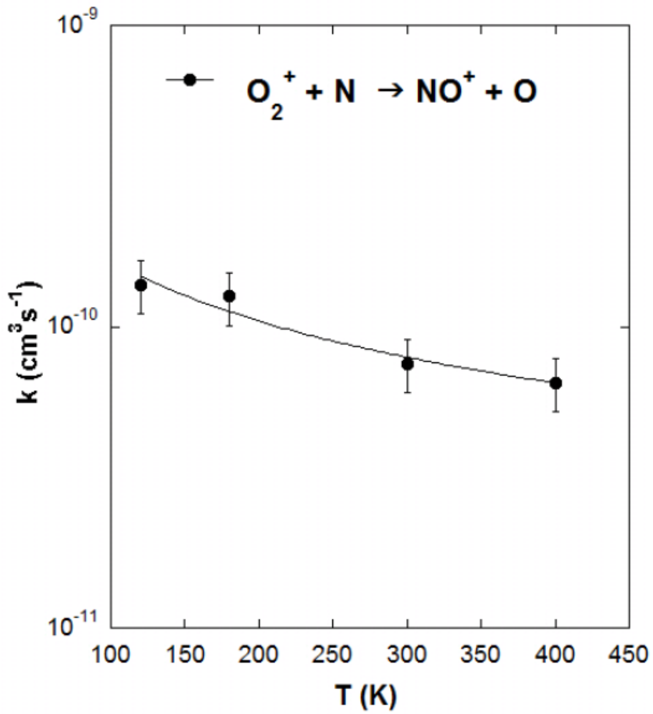

J. Chem. Phys. **142** DOI: 154305 (Apr 2015)

Negative Ion - Atom Results

$$O_2^- + N \rightarrow NO_2 + e^-, \quad \Delta_r H^\circ = -4.11\,\text{eV},$$

$$NO + O^-, \quad \Delta_r H^\circ = -2.39\,\text{eV},$$

$$O_2^- + O \rightarrow O_3 + e^-, \quad \Delta_r H^\circ = -0.66\,\text{eV},$$

$$O_2 + O^-, \quad \Delta_r H^\circ = -1.01\,\text{eV},$$

$$O^- + N \rightarrow NO + e^-, \quad \Delta_r H^\circ = -5.09\,\text{eV},$$

$$O^- + O \rightarrow O_2 + e^-, \quad \Delta_r H^\circ = -3.71\,\text{eV}.$$

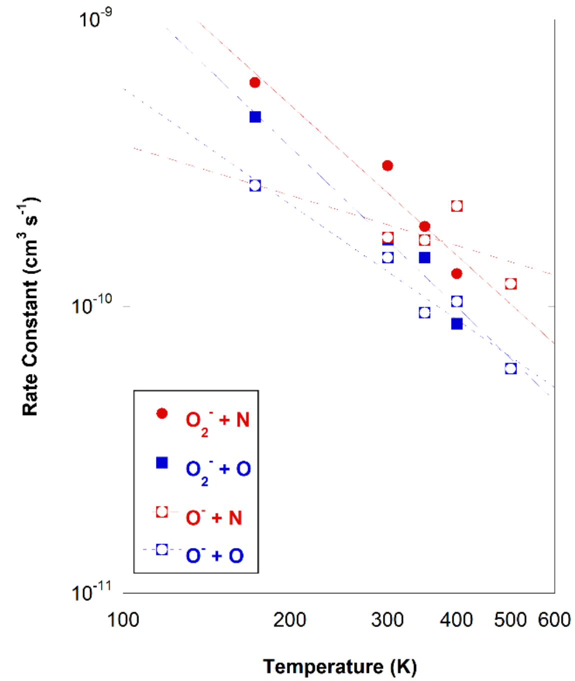

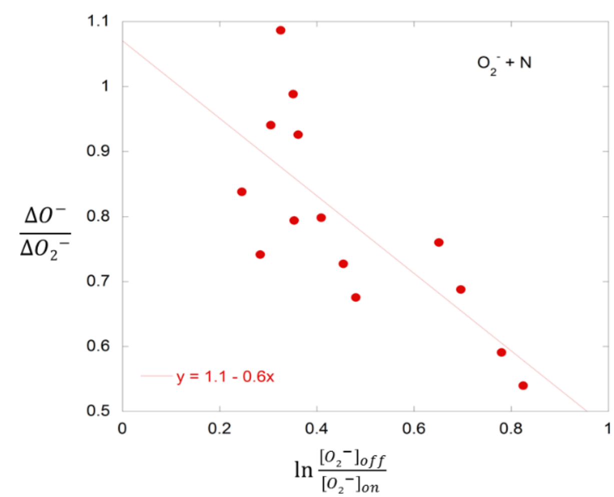

J. Chem. Phys. **139**, 144302,
doi: 10.1063/1.4824018 (Oct 2013)

Turbulent Ion Flow Tube

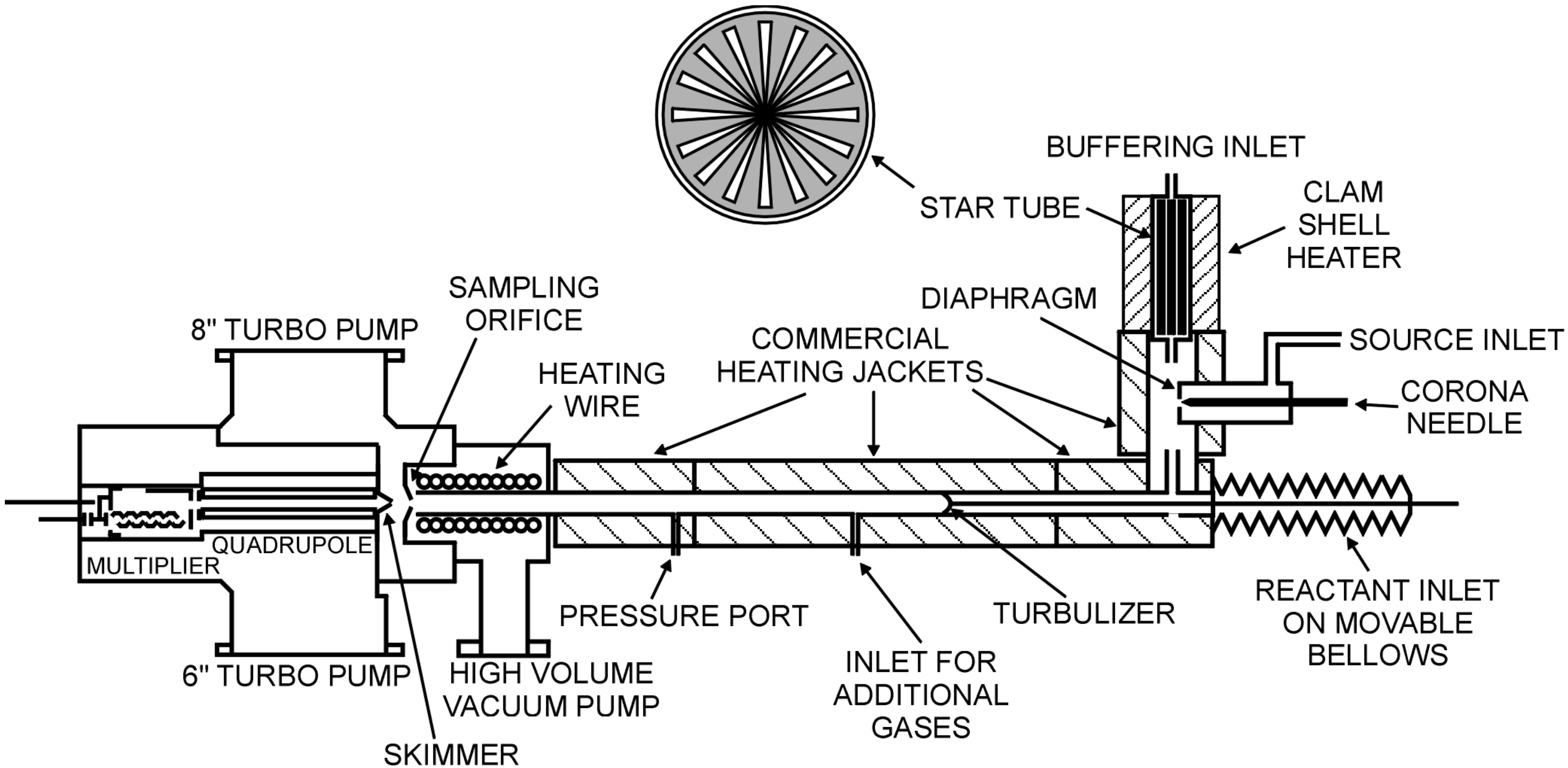

10-760 Torr

300-700 K

Also for very slow rate constants

Limits for O_2^+ with N_2

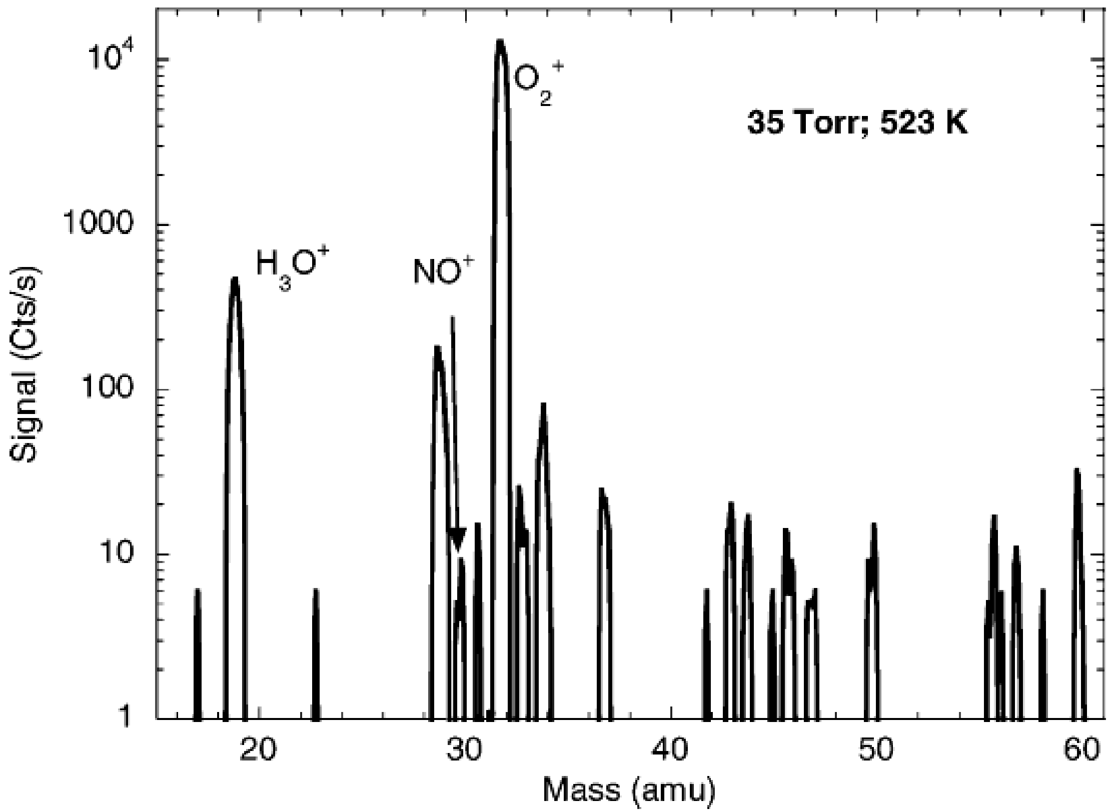

Figure 1. Mass spectrum taken at 35 Torr and 523 K.

T (K)	k (upper limit)
423	$2x10^{-21}$
523	$4x10^{-21}$
623	$1x10^{-20}$

J. Phys. Chem. A **110** 11599-11601(Oct 2006)

$O_2(a\ ^1\Delta_g)$ background

- **$O_2(a\ ^1\Delta_g)$ emissions at 1270 nm contribute to the IR airglow[1]**
- **$O_2(a\ ^1\Delta_g)$ created in O_2 discharges[2]**
  - **Electron impact on O_2**
  - **$O_2(b\ ^1\Sigma_g^+)$ collisional quenching by O_2**
- **Affects oxidation chemistry**
  - **Materials processing[3]**
  - **Oxygen-iodine lasers[4]**

[1]*Handbook of Geophys. & Space Environ.,* A.S. Jursa, ed. 1985.

[2]Scweitzer and Schmidt, *Chem. Rev.* **103**, 1685-1757 (2003)

[3]Jeong et al., *Plasma Sources Sci. Technol.* **7**, 282-285 (1998)

[4]A. P. Naparatovich et al., *J. Phys. D: Appl. Phys.*, **34**, 1827 (20

$O_2(a\ ^1\Delta_g)$ in Ionosphere D-region

- **Reactions controlling e- concentrations in ionosphere influence radiowave propagation[1]**

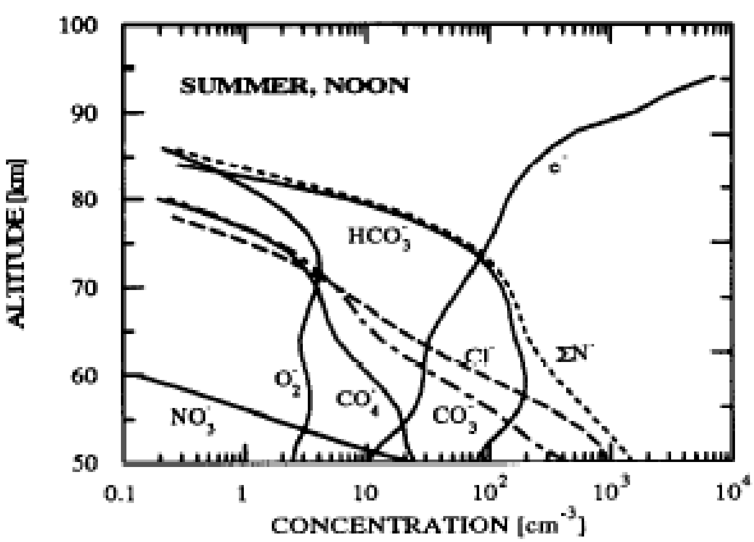

Brasseur and DeBats, *JGR*, **91**, 4025 (1985)

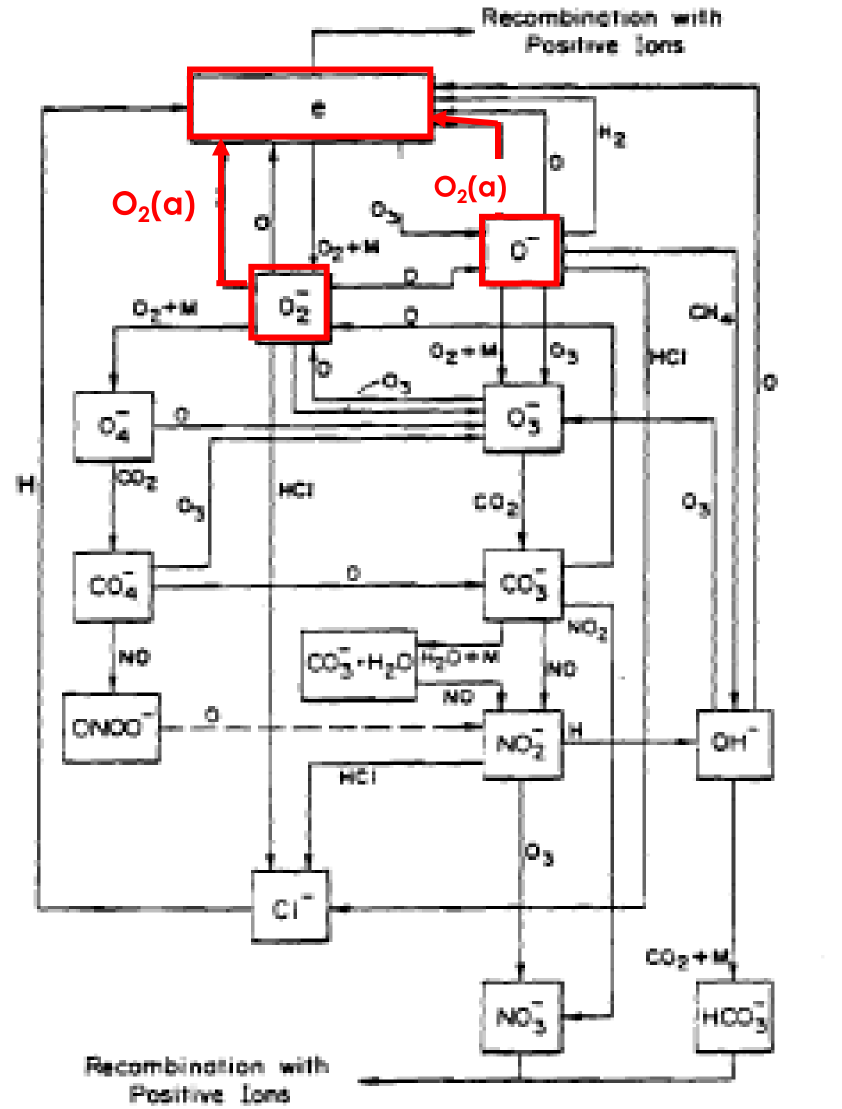

[1]*Handbook of Geophys. & Space Environ.,* A.S. Jursa, ed. 198

Previous Kinetics for $O_2(a\,^1\Delta_g)$ Reactions

- **Large disparity in the literature values of the rate constants for O^- and O_2^- + $O_2(a\,^1\Delta_g)$**
- **O_2^- + $O_2(a\,^1\Delta_g)$**
  - **NOAA flowing afterglow (FA)[10]** — **2.0×10^{-10} cm^3 s^{-1}**
  - **Upschulte et al., FA[11]** — **2.4×10^{-11} cm^3 s^{-1}**

[11] *JPC.* **98**, 837 (1994)

- **O^- + $O_2(a\,^1\Delta_g)$:**
  - **NOAA, FA** — **3.0×10^{-10} cm^3 s^{-1}**
  - **Upschulte et al., FA** — **3.3×10^{-11} cm^3 s^{-1}**
  - **Belostostky et al., plasma model** — **1.9×10^{-10} cm^{3}s^{-1}**
  - **Stoffels et al., plasma model** — **1.3×10^{-10} cm^3 s^{-1}**

AFRL Experiments

- **Utilize newly designed $O_2(a\ ^1\Delta_g)$ emission detection scheme to re-measure the kinetics for the O^-, O_2^- + $O_2(a\ ^1\Delta_g)$ reactions from 200-700 K**
- **Calibrate detection setup vs. absolute standard**
  - **Settle the discrepancy in the literature values**
- **Expand the studies to other ion-molecule reactions with $O_2(a\ ^1\Delta_g)$**

J. Phys. Chem. A. **111, 5218-5222 (June 2007)**

J. Phys. Chem A **112, 3040-3045 (Apr 2008)**

SIFT with $O_2(a\ ^1\Delta_g)$ Detection
Initial experiments

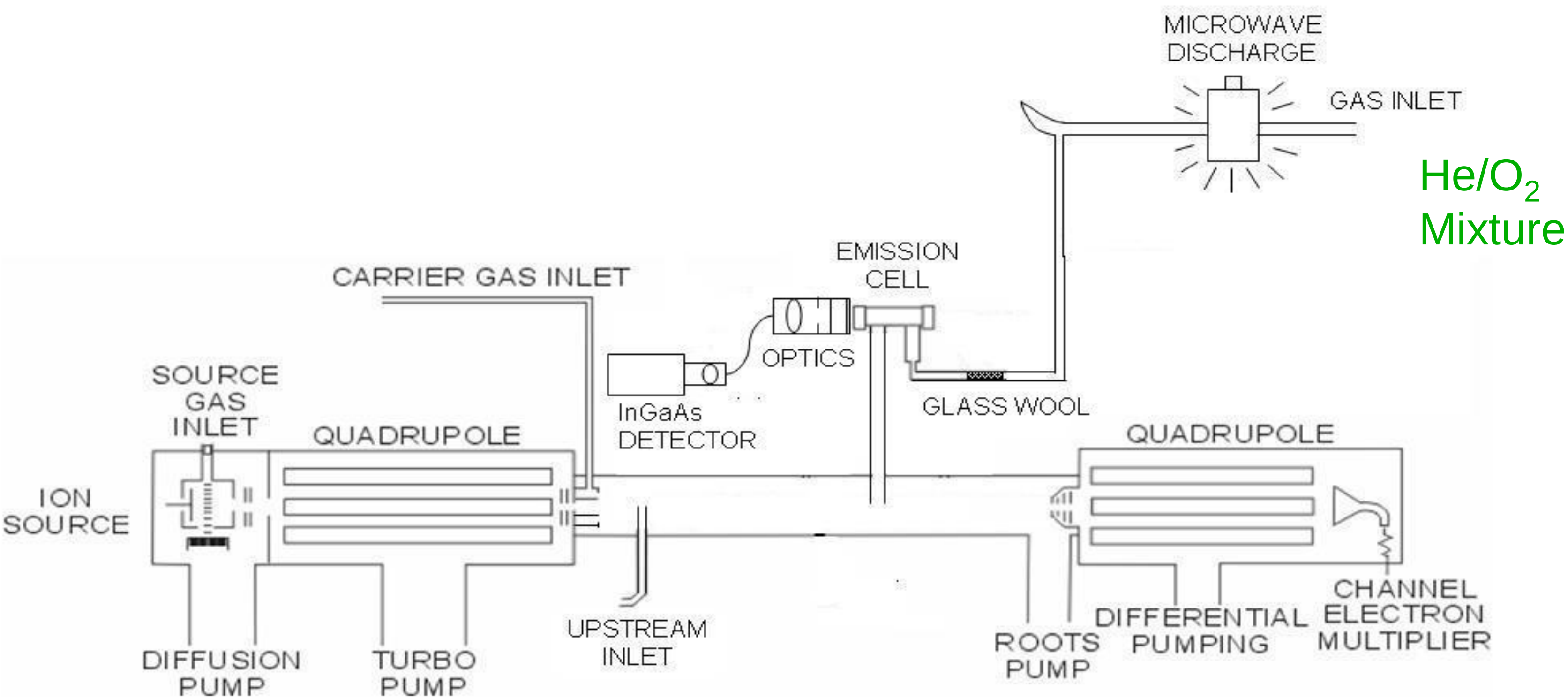

Glass wool: quenches most O atoms from discharge

<u>Typical % of total O_2 concentration in SIFT</u>: 9% $O_2(a\ ^1\Delta_g)$, 1% O, <1% O_3

Chemical $O_2(a\ ^1\Delta_g)$ Generation Can Study Temperature Dependencies

$$H_2O_2 + Cl_2 + 2KOH \rightarrow O_2/O_2(a) + 2KCl + 2H_2O$$

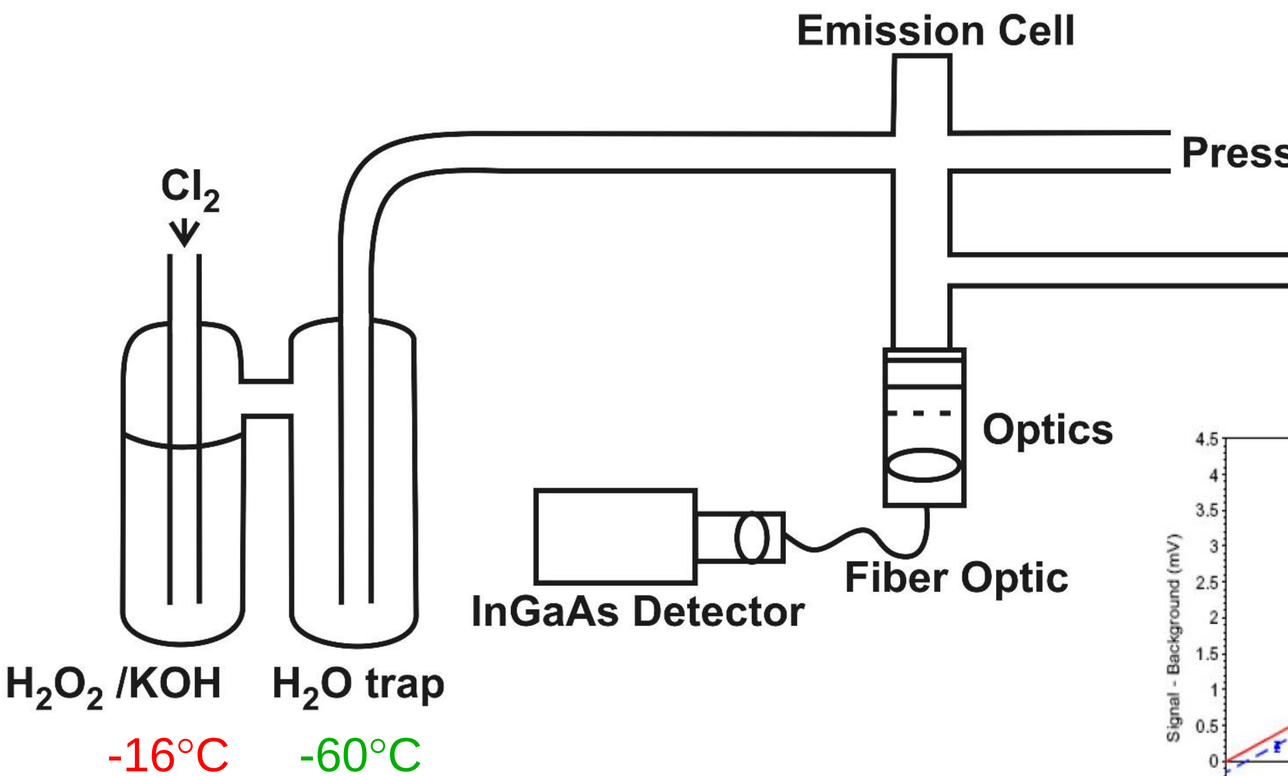

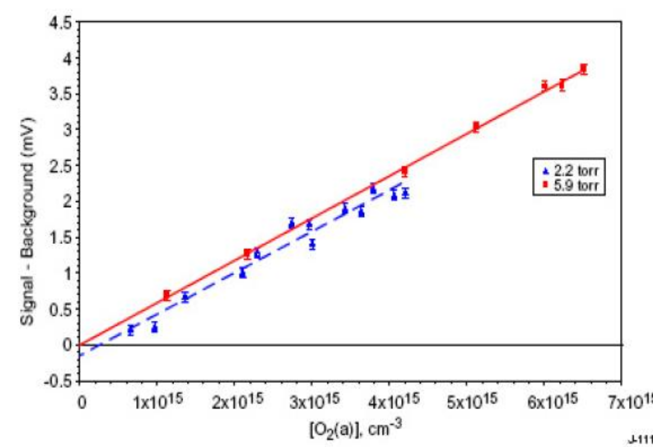

$O_2^- + O_2(a\ ^1\Delta_g) \rightarrow 2O_2 + e^-$

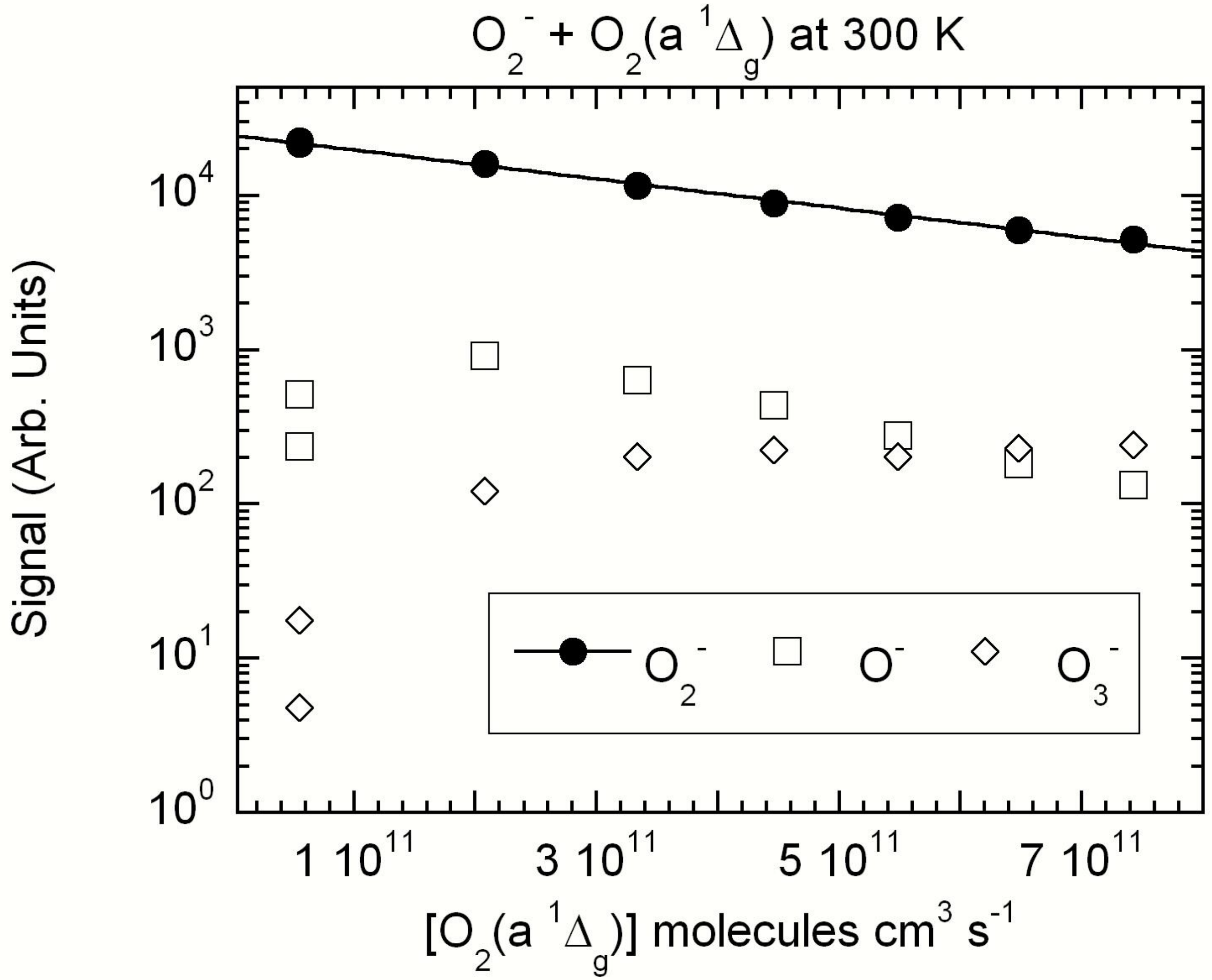

Need to account for O, O_3 impurities

$O_2^- + O_2(a\ ^1\Delta_g)$ 298 K Results

- $k = 6.6 \times 10^{-10}\ cm^3\ s^{-1}$
  - 90% of collision rate constant ∴ very efficient
  - 3x higher than previous highest values
- Upshulte et al. FA experiments
  - Kinetics data showed fast and slow decay
  - Incorrectly assumed slow decay was correct
    - New bi-exponential fit shows fast decay = NOAA value
  - O_2 source gas present in FA flow tube
    - Electrons present re-attach to O_2 ∴ lower apparent decay in FA measurements

$O^- + O_2(a\ ^1\Delta_g)$ 298 K Results

- k = 1.1×10^{-10} cm^3 s^{-1}
  - 12% of $k_{col}=9.0\times10^{-10}$ cm^3 s^{-1}
  - 2-3x < previous values (even more – see T work)
- New charge transfer product channel observed:

$$O^- + O_2\left(a\ ^1\Delta_g\right) \rightarrow O_3 + e + 60\ \text{kJ mol}^{-1} \qquad <70\%$$

$$\rightarrow O_2^- + O + e - 3\ \text{kJ mol}^{-1} \qquad >30\%$$

- New channel important pathway in low-pressure O_2 discharges where:
  - O^- is primary ion
  - Three-body O_2^- formation negligible

Temperature Dependencies
200-700 K

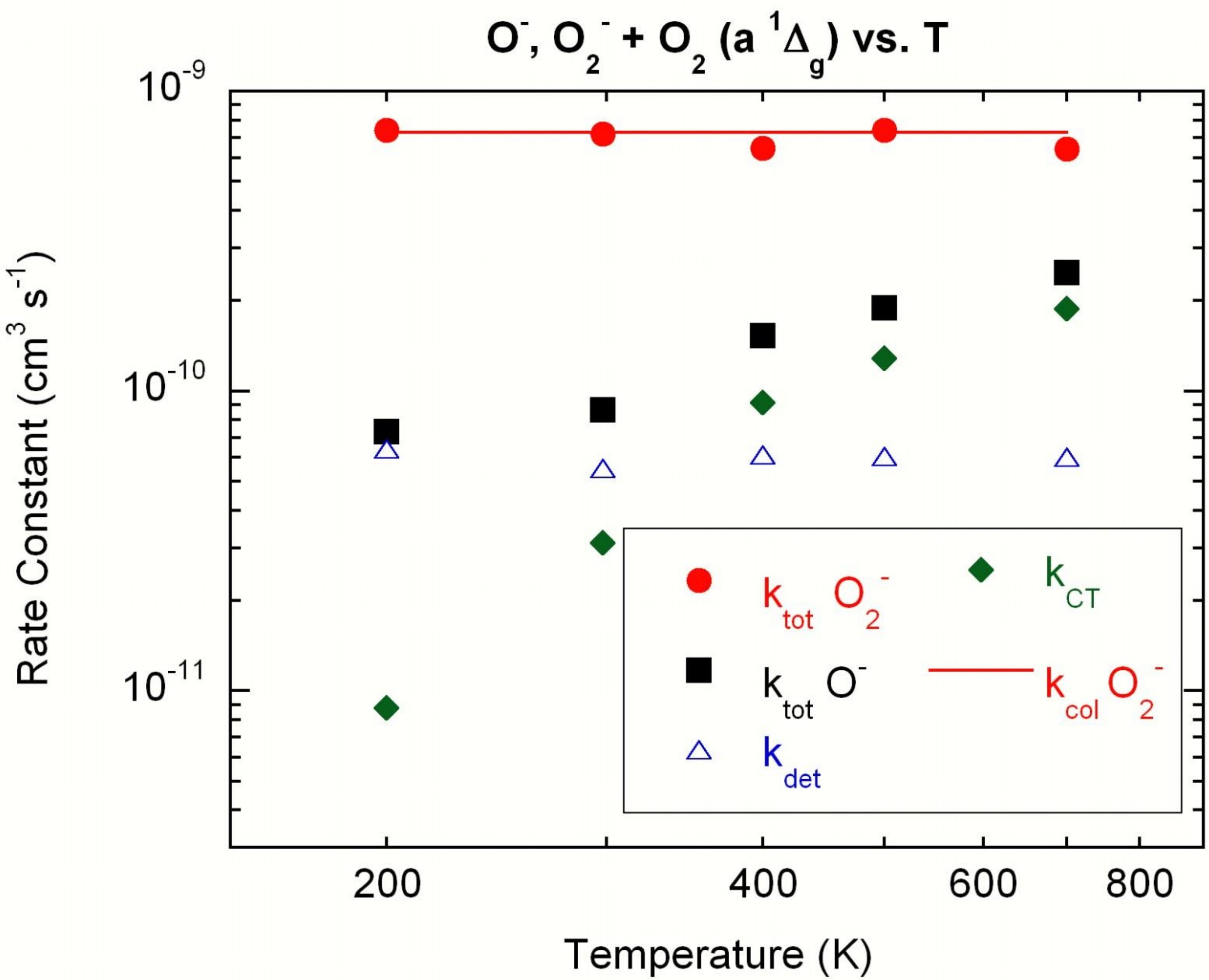

Implications for Models
Temperature Dependencies

- O^- rate constant at 298 K = 8.6×10^{-11} cm^3 s^{-1}

- D-region is cold ∴ O^- rate constants are lower than previously assumed at low temperatures given positive *T* dependence

- Increased fraction of O^- converted to O_2^- at high temperatures increases conversion rate to electrons
  - Additional O_2^- rapidly converted to e^-

Conclusions

Innovative techniques allow wide range of species studied

New techniques often yield unexpected results

Acknowledgments

In-house

Tom Miller

Skip Williams

Bob Morris

Sue Arnold

Nick Shuman

Shaun Ard

Oscar Martinez

Justin Wiens

Jenny Sanchez

Theory

E. Mishin - atmospheric modeling

Jurgen Troe – statistical modeling

Made possible by long term funding by AFOSR Molecular Dynamics (Berman)